On GA Optimized Automatic Generation Control with Superconducting Magnetic Energy Storage

EMIL NINAN SKARIAH
Department of Electrical and Electronics Engineering
SAINTGITS College of Engineering
Pathamuttom P.O., Kottayam
INDIA
emil.skariah@gmail.com

RAJESH JOSEPH ABRAHAM
Department of Avionics
Indian Institute of Space Science and Technology
Valiamala P.O., Thiruvananthapuram,
INDIA
rajeshja@gmail.com

Abstract: - This paper discusses the effect of a Superconducting Magnetic Energy Storage (SMES) on low frequency oscillations in area frequency deviations and the tie line power variations following a step load perturbation. A two area interconnected thermal power system with two reheat generating units in area 1 and two non reheat generating units in area 2 has been considered with SMES unit in each area. The optimal integral gain settings of both the areas without and with SMES are obtained for different combinations of ACE participation factors using Genetic Algorithm where the objective function considered is quadratic in frequency deviations and tie line power deviations. A comparison of dynamic performances without and with SMES units reveals that SMES can effectively improve the dynamic responses by reducing the overshoots and settling time to a significant extent.

Key-Words: - Automatic Generation Control, Genetic Algorithm, Integral Squared Error technique, Superconducting Magnetic Energy Storage.

1 Introduction

Automatic Generation Control (AGC) has been one of the most debated topics ever since the operation of interconnected power systems began [1-8]. One of the main tasks involved in reliable and efficient interconnected power system operation is to maintain the interchanged power and the system frequency at their respective scheduled values so that the power system remains at its nominal state characterized by nominal system frequency, voltage profile and load flow configuration. For this, the generated power should instantaneously match the demanded power and associated power losses. Since the load is continuously changing, it is practically impossible to attain perfect power generation - consumption equilibrium and the resulting mismatch is reflected as deviations in system frequency and tie line power flows from their respective scheduled values. Relatively close control of frequency ensures constancy of speed of induction and synchronous motors. Constancy of speed of motors drives is particularly important for satisfactory performance of generating units as they are highly dependent on the performance of all the associated auxiliary drives. Thus AGC of an interconnected power system is concerned with two main objectives: instantaneously matching the generation to the system load and adjusting the system frequency and tie line loadings at their scheduled values as close as possible so that, the quality of the power delivered is maintained at requisite level.

A review of literature shows that most of the works concerned with AGC pertain to tie line power control strategy [9-14]. This is realized by regulating the area control errors to zero using supplementary control. Integral controllers have been used for the supplementary control in AGC. Even in the case of small load disturbances and with the optimized gain for the supplementary controllers, the power frequency and tie line power deviations persist for a long duration. In these situations, the governor system may no longer be able to absorb the frequency fluctuations due to its slow response. Thus a limit is imposed on the degree to which frequency deviations and tie line power deviations can be minimized, since the inertia of the rotating parts is the only energy storage capacity in a power system.

To compensate for the sudden load changes, an active power source with fast response such as a Superconducting Magnetic Energy Storage (SMES) unit is expected to be the most effective countermeasure [15-20]. Thus SMES can improve power quality and improve system operation in terms of frequency regulation, reduction of area

control error and inadvertent tie line flow. Compared with other active energy sources, SMES has inherent advantages that it has fast response in the range of milliseconds and it acts almost as a lossless storage device. No energy conversion is needed and so higher efficiency is ensured. These systems are capable of providing instantaneous reserves for rapidly changing loads and can effectively reduce the frequency deviations and tie line power deviations due to small load disturbances. Oscillations in frequency deviations and tie line power deviations are also damped out. SMES also has other applications in power systems like system stability improvement, spinning reserve, VAR control, power quality improvement etc.

Owing to the developments in computer technologies and recent development of parallel computing environments, Genetic Algorithms (GA) are emerging as powerful alternatives to traditional optimization methods which are CPU intensive [21-24]. GA is one of the most advanced forms of evolutionary computation techniques which have been highly successful for getting computers to automatically solve problems without having to tell them explicitly how. GA's are global search algorithms based on the natural law of evolution of species by natural selection. Few fundamental characteristics that make GA versatile, flexible and applicable to a wide range of optimization problems are that, GA's are blind search methods which uses information only about objective function, they are parallel search schemes which simultaneously evaluate many points in the parameter space rather than a single point, they work directly with bit strings representing the parameter sets and not the parameter themselves etc.

In view of the above, this paper aims to investigate the effect of SMES units on the dynamic performances of an interconnected thermal power system following a step load disturbance in either of the areas. For different ACE participation factors, the optimum values of integral gain settings in the control areas without and with SMES units are obtained using Genetic algorithms.

2 AGC System Model studied

A two area interconnected power system has been considered for the present work. Area 1 consists of two reheat generating units and area 2 consists of two non reheat generating units. In either of the areas, both generators are assumed to form a coherent group. A schematic of the power system under analysis is given in Fig.1.

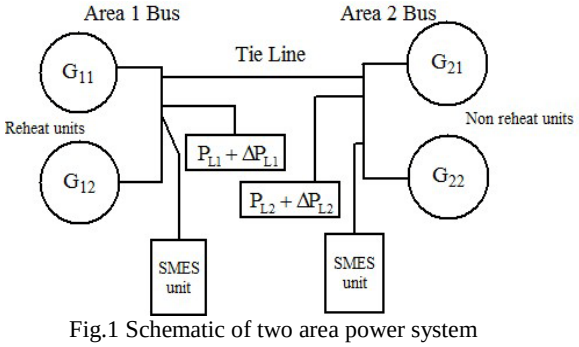

Fig.1 Schematic of two area power system

Since thermal units are subjected to thermodynamic and mechanical stresses, there is a limit to the rate at which the turbine output can be changed. This limit is termed as generation rate constraint and a limit of 3% per minute for reheat units and 10% per minute for non reheat units are considered [25]. Supplementary integral control is the conventional control employed in each area to minimize the respective area control error to zero thereby reducing the frequency deviations and tie line power deviations. The input to the integral controller in each area is the respective Area Control Error (ACE) signal, which is a linear combination of the frequency perturbation and tie-line power deviation. Since small load perturbations are considered in the AGC problem, a small perturbation transfer function model is being used for the studies as shown in Fig.2. The two areas are interconnected by tie line and the load demands are to be shared by the two units in each of the areas according to their respective ACE participation factors. apf_{11} and apf_{12} are the ACE participation factors in area 1 whereas apf_{21} and apf_{22} are the ACE participation factors in area 2. In area 1, $apf_{11} + apf_{12} = 1$ and in area 2, $apf_{21} + apf_{22} = 1$. Small capacity SMES units are connected in each of the areas. A step load disturbance of 1% in either of the areas has been considered for the investigations.

The state space equations governing the system are:

Area 1

$$\Delta \dot{f}_1 = \frac{-1}{T_{p1}}\Delta f_1 + \frac{K_{p1}}{T_{p1}}\Delta P_{g1} + \frac{K_{p1}}{T_{p1}}\Delta P_{g2} - \frac{K_{p1}}{T_{p1}}\Delta P_{tie12} - \frac{K_{p1}}{T_{p1}}\Delta P_{d1} \quad (1)$$

$$\Delta \dot{P}_{g1} = \frac{-1}{T_{R1}}\Delta P_{g1} + \left(\frac{1}{T_{R1}} - \frac{K_{R1}}{T_{T1}}\right)\Delta P_{t1} + \frac{K_{R1}}{T_{T1}}\Delta P_{r1} \quad (2)$$

$$\Delta P_{t1} = \frac{-1}{T_{T1}}\Delta P_{t1} + \frac{1}{T_{T1}}\Delta \Pr 1 \quad (3)$$

$$\Delta \dot{P}_{r1} = \frac{-1}{T_{G1}R_1}\Delta f_1 - \frac{1}{T_{G1}}\Delta P_{r1} + \frac{apf_{11}}{T_{G1}}u_1 \quad (4)$$

$$\Delta \dot{P}_{g2} = \frac{-1}{T_{R2}}\Delta P_{g2} + \left(\frac{1}{T_{R2}} - \frac{K_{R2}}{T_{T2}}\right)\Delta P_{t2} + \frac{K_{R2}}{T_{T2}}\Delta P_{r2} \quad (5)$$

$$\Delta \dot{P}_{t2} = \frac{-1}{T_{T2}} \Delta P_{t2} + \frac{1}{T_{T2}} \Delta P_{r2} \quad (6)$$

$$\Delta \dot{P}_{r2} = \frac{-1}{T_{G2} R_2} \Delta f_1 - \frac{1}{T_{G2}} \Delta P_{r2} + \frac{apf_{12}}{T_{G2}} u_1 \quad (7)$$

$$\Delta \dot{P}_{tie12} = 2\Pi T_{12} \left(\Delta f_1 - \Delta f_2 \right) \quad (8)$$

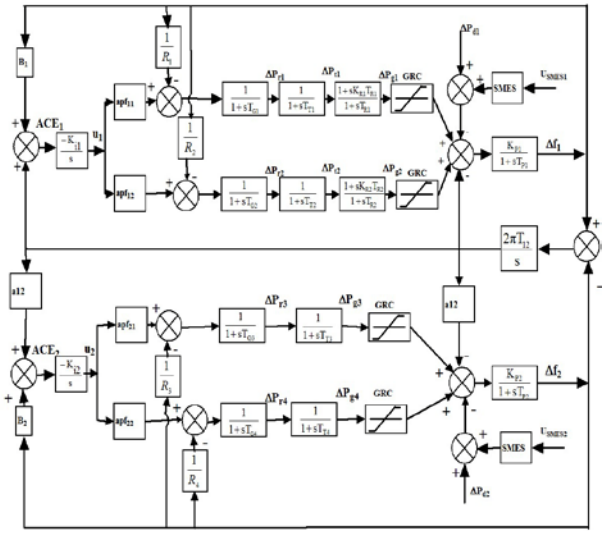

Fig.2 Two area interconnected power system model with SMES units

Area 2

$$\Delta \dot{f}_2 = \frac{-a_{12} K_{P2}}{T_{P2}} \Delta P_{tie12} - \frac{1}{T_{P2}} \Delta f_2 + \frac{K_{P2}}{T_{P2}} \left(\Delta P_{g3} + \Delta P_{g4} - \Delta P_{d2} \right) \quad (9)$$

$$\Delta \dot{P}_{g3} = \frac{1}{T_{T3}} \left(\Delta P_{r3} - \Delta P_{g3} \right) \quad (10)$$

$$\Delta \dot{P}_{r3} = \frac{-1}{T_{G3} R_3} \Delta f_2 - \frac{1}{T_{G3}} \Delta P_{r3} + \frac{apf_{21}}{T_{G3}} u_2 \quad (11)$$

$$\Delta \dot{P}_{g4} = \frac{1}{T_{T4}} \left(\Delta P_{r4} - \Delta P_{g4} \right) \quad (12)$$

$$\Delta \dot{P}_{r4} = \frac{-1}{T_{G4} R_4} \Delta f_2 - \frac{1}{T_{G4}} \Delta P_{r4} + \frac{apf_{22}}{T_{G4}} u_2 \quad (13)$$

which can be represented by the standard state space model,

$$\dot{X} = AX + BU + \Gamma P \quad (14)$$

where X, U and P are the state, input and disturbance vectors given by

$X^T = [\Delta f_1 \ \Delta P_{g1} \ \Delta P_{t1} \ \Delta P_{r1} \ \Delta P_{g2} \ \Delta P_{t2} \ \Delta P_{r2} \ \Delta P_{tie12} \ \Delta f_2 \ \Delta P_{g3} \ \Delta P_{r3} \ \Delta P_{g4} \ \Delta P_{r4}]$ (15)

$U^T = [U_1 \ U_2]$ (16)

$P = [\Delta Pd1 \ \Delta Pd2]$ (17)

while A, B, and Γ are real constant coefficient matrices associated with the corresponding vectors respectively. The system parameters are presented in Appendix.

3 Superconducting Magnetic Energy Storage Unit

SMES is a technology based on the ability of superconductors to carry high dc currents with no resistive loss in the presence of significant magnetic fields, thereby directly storing electrical energy. Its advantage is that it is capable of providing instantaneous supply or demand of power [14-20]. SMES units consist of a dc magnetic coil kept in superconducting medium, a power conditioning system and the control circuit. The inductor coil conducts with virtually zero losses as the heat generated is transferred to the refrigerating medium, usually liquid helium. An alloy of niobium and titanium is usually used for the superconducting coil. Low temperatures at the ranges of 4 to 10K are maintained by the refrigerant. Hence energy will be stored as magnetic field provided by the circulating current in the coil. Stored energy in the coil is given by

$$w = \frac{1}{2} L I_d^2 \quad (18)$$

where w is the energy in joules, L is the inductance of the coil and I_d is the inductor current. SMES units have been used as an efficient aid for control and regulation of power systems. The circuit diagram of SMES is shown in Fig. 3 in which a dc magnetic coil is connected to ac grid through a power conversion system (PCS) which includes an inverter/rectifier. Power conversion system is used for the energy exchange between SMES coil and the ac grid and it has a wye-delta connected transformer arrangement and a 12-pulse line commutated converter. The energy exchange between the superconducting coil and the electric power system is controlled by the line commutated converter. The particular transformer arrangement and higher pulse number of the converter circuit ensures harmonics being intruded into the ac grid are reduced. The voltage across the inductor can be varied over a range of positive and negative values by varying the firing angle of SCR's from 0^0 to 180^0. The dc voltage across the inductor in kV is given by [26].

$$E_d = 2V_{d0} Cos\alpha - 2I_d R_C \quad (19)$$

where α is the firing angle in degrees, Id is the current flowing through the inductor in kA, RC is the equivalent commutating resistance in kΩ and Vd0 is the maximum circuit bridge voltage in kV. The inductor is first charged to a set value by

applying a positive voltage Ed. As the inductor current attains its set value, the voltage across it is reduced to zero.

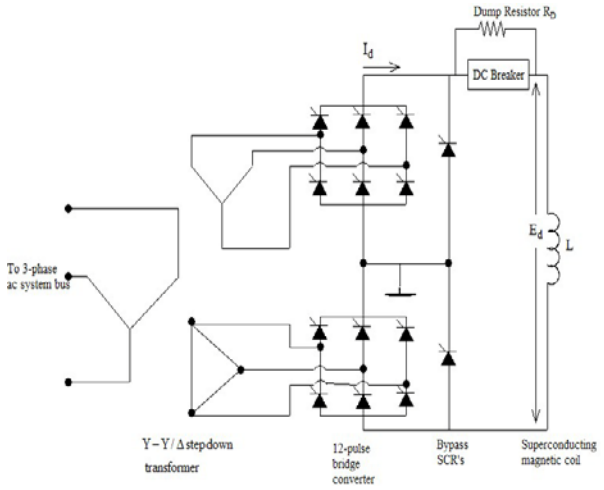

Fig.3 SMES Circuit diagram

The current circulates in the coil virtually without losses as it is kept in the cryogenic medium. Hence energy is stored as magnetic field in the SMES coil. The coil is now ready for its intended function in the power system to which it is linked through the power conditioning system. When there is a sudden power demand in the power system, it is met by the action of governing system which increases the mechanical power input accordingly. These conventional control actions take seconds to complete. As an SMES coil is augmented with the power system, the power demand is instantaneously supplied from its stored energy before the governor control comes into play. Similarly, for excess power in the system, it will be absorbed by the SMES coil. As the conventional governor control actions dominate after few seconds, the SMES coil gets charged or discharged to its previously set value. When $\alpha < 900$, converter acts in converter mode (charging mode) and when $\alpha > 900$, converter acts in inverter mode (discharging mode).

4 SMES Control Strategy

For a sudden load demand, the frequency will fall resulting in a negative value of frequency deviation. This will reflect as a negative voltage across the coil and hence the required energy will be discharged to the ac grid. For excess power in the system, a positive voltage will be impressed across the inductor and energy will be absorbed from the ac grid. Frequency deviation Δf_i is taken as the control signal for SMES unit in the ith area.

The incremental change in inductor voltage for the SMES unit in the ith area is,

$$\Delta E_{d_i} = \left[\frac{K_{SMES_i}}{1+sT_{DC_i}}\right]\Delta f_i \qquad ; i = 1, 2 \tag{20}$$

where, ΔE_{di} is the incremental change in converter voltage; T_{DCi} is the converter time delay; K_{SMESi} is the gain of the SMES unit and Δf_i is the frequency deviation. The fall or deviation in inductor current is given by,

$$\Delta I_{d_i} = \frac{\Delta E_{d_i}}{sL_i} \tag{21}$$

While following Eqn.(21), the relationship Power flow into the inductor at any time is $P_d = E_d.I_d$ and the initial power flow into the coil is $P_{d0} = E_{d0}.I_{d0}$ where E_{d0} and I_{d0} are the magnitudes of voltage and current prior to the load disturbance. When a load disturbance occurs, the power flow into the coil can be expressed as:

$$P_{d0} + \Delta P_d = \left(E_{d0} + \Delta E_d\right)\left(I_{d0} + \Delta I_d\right) \tag{22}$$

and hence the incremental power change in the inductor is:

$$\Delta P_d = I_{d0}\Delta E_d + \Delta E_d \Delta I_d \tag{23}$$

The term $E_{d0}\Delta I_d$ is neglected as $E_{d0} = 0$ in the storage mode to hold the rated current at constant value. Thus the incremental change in inductor power flow per unit is given by:

$$\Delta P_d = \left(I_{d0}\Delta E_d + \Delta E_d \Delta I_d\right)/\, P_R \tag{24}$$

5 Inductor Current Deviation Feedback

The natural restoration of inductor current to its rated value is a slow process and the rate of current restoration has to be improved by alternate methods. The inductor current has to be restored to its rated value quickly as possible such that it can respond to the next load disturbance effectively. To improve the current restoration rate to its steady state value, a feedback loop is employed in the SMES control loop by applying a negative feedback with inductor current deviation signal. The incremental change in inductor voltage is then,

$$\Delta E_{d_i} = \frac{1}{1+sT_{DC_i}}\left[K_{SMES_i}(\Delta f_i) - K_{id}\Delta I_{d_i}\right] \quad (25)$$

where K_{id} is the gain of negative current feedback ΔI_{di}. The SMES unit with negative induction current deviation feedback is shown in Fig.4.

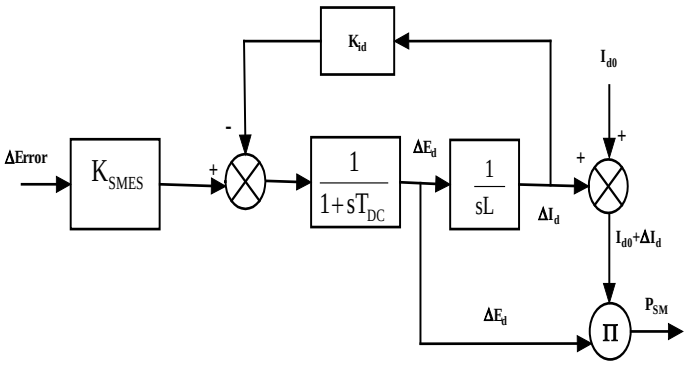

Fig.4 SMES Block diagram with negative inductor current deviation feedback

6 Genetic Algorithm Optimized Integral Gain Settings

The efficiency of supplementary control is determined by the optimal integral gain settings K_{i1} and K_{i2} of area 1 and area 2 respectively. The optimum values of integral gains are obtained using genetic algorithm (GA). An initial population of gain values is first created which are coded as bit strings called chromosomes. Each of these chromosomes represents a possible solution of optimization. GA operations such as selection, crossover and mutation are performed on the population. GA searches not on single points as in traditional optimization methods but many points in the search space. In each iteration, fitness value of each individual is calculated and the best parents are selected. These parents are combined with each other (crossover) or within themselves (mutation) to produce offsprings for the next generation. As the number of generations advances, the program evolves to an optimal solution. The algorithm gets stopped when the prescribed stopping criteria is met. The schematic of genetic algorithm in AGC problem is shown in Fig.5.

An objective function based on the Integral Square Error technique is considered and the corresponding performance index is minimized for 1% step load disturbance in either of the areas keeping the other area uncontrolled following the approach of [8]. The quadratic performance index is,

$$J = \int_0^t \left(w_1\Delta f_1^{\,2} + w_2\Delta f_2^{\,2} + w_3\Delta P_{tie12}^2\right) \quad (26)$$

where w_1, w_2 and w_3 are the respective weighting factors. The optimal values of K_{i1} and K_{i2} which minimizes J with 1% step load perturbation in either of the areas are obtained for different area participation factors with and without the presence of SMES units in the power system studied and are given in Tables 1 and 2 respectively.

Following [8], the optimal gain settings K_{i1} for area 1 are obtained on an individual basis by keeping area 2 uncontrolled. Similarly optimal values of integral gain settings (K_{i2}) for area 2 are obtained by keeping area 1 uncontrolled.

Table:1 Optimal integral gain values for area 1 (K_{i1}) with 1% step load perturbation in area 1

apf_{11}	apf_{12}	Gain Values	
		Without SMES units	With SMES units
0.1	0.9	0.5735	1.4275
0.25	0.75	0.9997	1.7092
0.5	0.5	0.3904	0.9831
0.75	0.25	0.9748	1.7092
0.9	0.1	0.5314	1.4210

Table:2 Optimal integral gain values for area 2 (K_{i2}) with 1% step load perturbation in area 1

apf_{11}	apf_{12}	Gain Values	
		Without SMES units	With SMES units
0.1	0.9	0.9918	1.999
0.25	0.75	0.9886	2.0
0.5	0.5	0.9864	1.9332
0.75	0.25	0.9941	2.0
0.9	0.1	0.9897	1.9998

7 Dynamic Responses and Discussion

Simulations are carried out in Matlab/Simulink version 7.6 environment to obtain the dynamic responses of the interconnected power system following 1% step load disturbance in either of the

control areas. The genetic algorithm options considered for simulation in this work are: Number of generations: 100, Population size: 50, Selection: Roulette wheel, Crossover: Single point, Mutation: Gaussian, Crossover probability: 0.98 and Elite count: 2. Fig. 6 shows the plot of fitness value versus number of generations for the integral gain setting K_{i1} of area 1 without SMES units. It implies that as the number of generation proceeds, the fitness value gets reduced and then reaches 0.07265, the minimum value of the performance index towards the end.

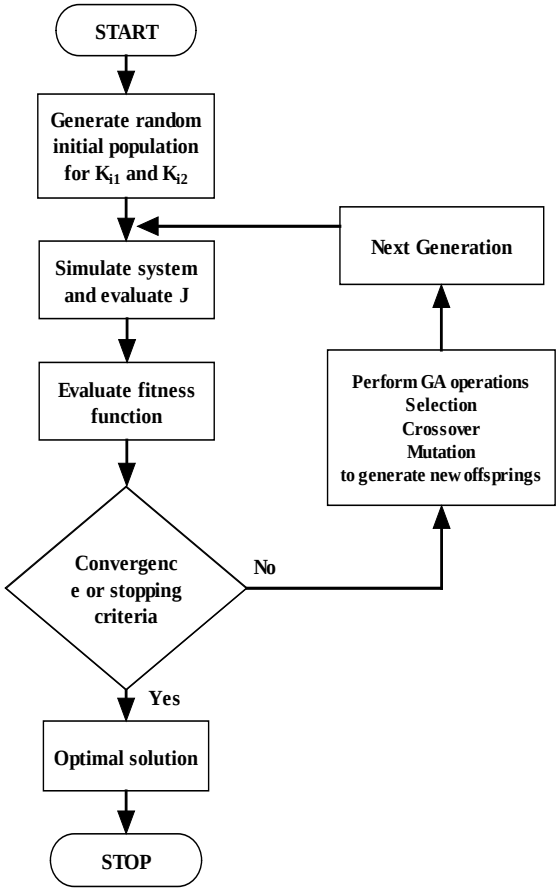

Fig.5 Schematic of GA in AGC

Different dynamic responses have been plotted in Figs. 7 to 12 for ACE participation factors $apf_{11} = apf_{12} = 0.5$ and $apf_{21} = apf_{22} = 0.5$. The frequency deviations and tie line power deviations with and without the presence of SMES units are shown in Fig.7.

It is observed that SMES units considerably reduce the peak overshoots and settling times of these responses. Owing to its fast response, SMES units meet the sudden load perturbations even before governor control actions come into play. This fast response of the SMES units is reflected in the plots showing deviations in frequency and interchanged power. It is also seen from Fig. 7 that the oscillations in frequency deviations in area1 and area 2 are damped out with the inclusion of SMES units. The low frequency oscillations in tie-line power deviation due to sudden load disturbance have also been suppressed effectively.

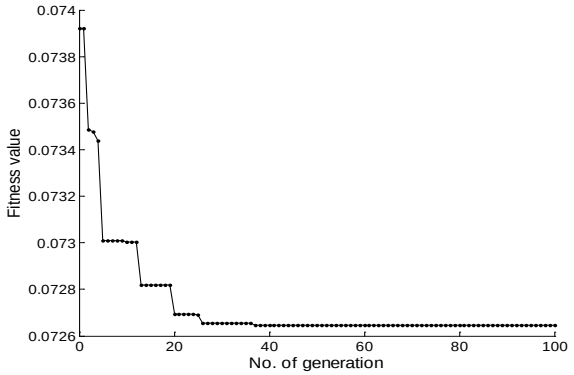

Fig.6 Convergence of genetic algorithm for K_{i1} optimization without SMES units

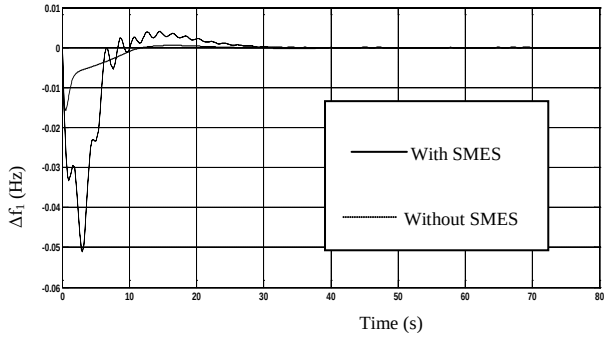

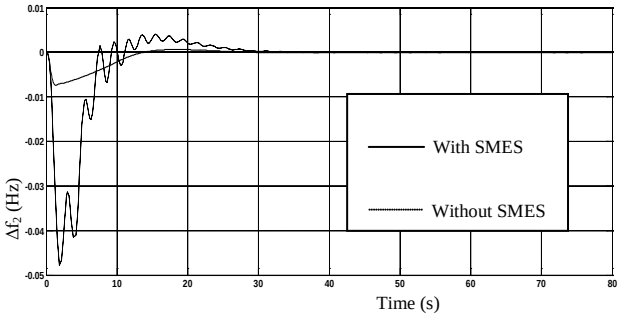

In automatic generation control, the load demanded in a particular control area is to be met by the generating units in that area itself. Thus, for a step load perturbation in area 1, generating units of area 1 should supply for the load demand while the incremental output of generating units in area 2 should settle down to zero as per the approved practices of automatic generation control.

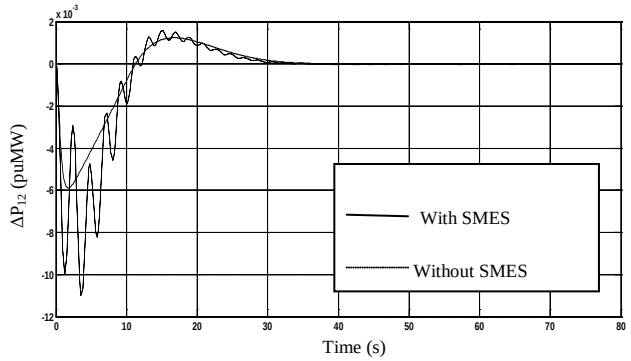

Fig.7 Dynamic responses for frequency deviations (Δf_1 & Δf_2) and tie line power deviations (ΔP_{tie12}) following 0.01 pu step load disturbance in area 1

The generation responses of the control areas with and without the presence of SMES are presented in Figs.8 and 9 with $apf_{11} = apf_{12} = 0.5$ in area 1 and $apf_{21} = apf_{22} = 0.5$ in area 2.

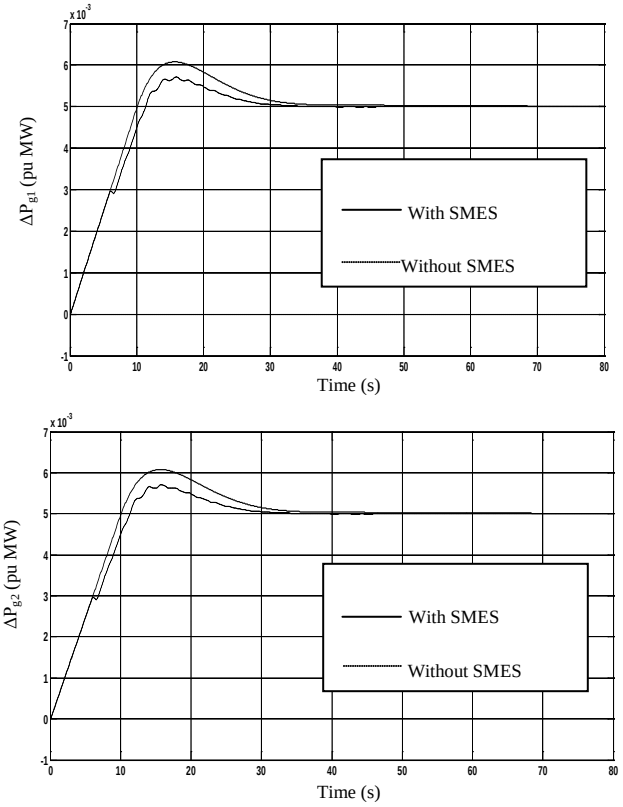

Fig. 8 Dynamic responses for ΔP_{g1} and ΔP_{g2} with 0.01 pu step load disturbance in area 1

Generating units contribute for the load perturbations in proportion to the corresponding ACE participation factors. i.e., $\Delta P_{G1} = apf_{11} \times 0.01 = 0.005$pu MW, $\Delta P_{G2} = apf_{12} \times 0.01 = 0.005$ pu MW and $\Delta P_{G3} = apf_{21} \times 0 = 0$ pu MW, $\Delta P_{G4} = apf_{22} \times 0 = 0$ pu MW.

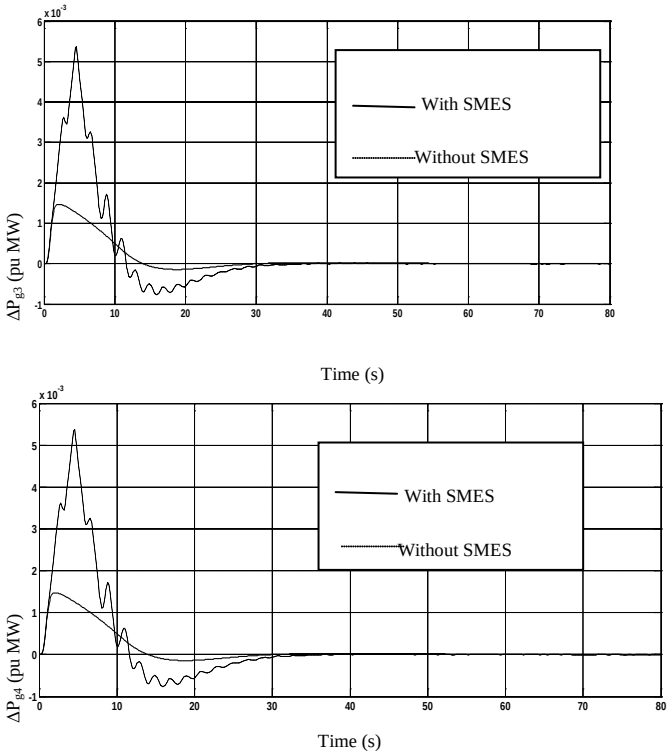

Fig.9 Dynamic responses for ΔP_{g3} and ΔP_{g4} with 0.01 pu step load disturbance in area 1

The generation responses of unit 1 and unit 2 settle down at 0.005 pu MW each, thus satisfying the load demand of 0.01 pu MW. The generating units 3 & 4 in area 2 does not contribute for this power demand as the disturbance is in area 1. It may be noted that, the peak oscillations and settling times which persist even after optimizing the supplementary controller has been reduced or suppressed to a considerable extent by the inclusion of SMES units.

Similar results are obtained with a step load disturbance of 0.01 pu MW in area 2. The frequency deviations and tie line power deviations are reduced to zero more effectively by the SMES action. The dynamic responses of frequency deviations and tie line power deviations are depicted in Fig.10.

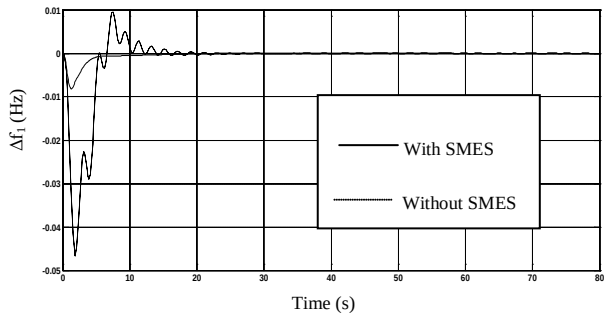

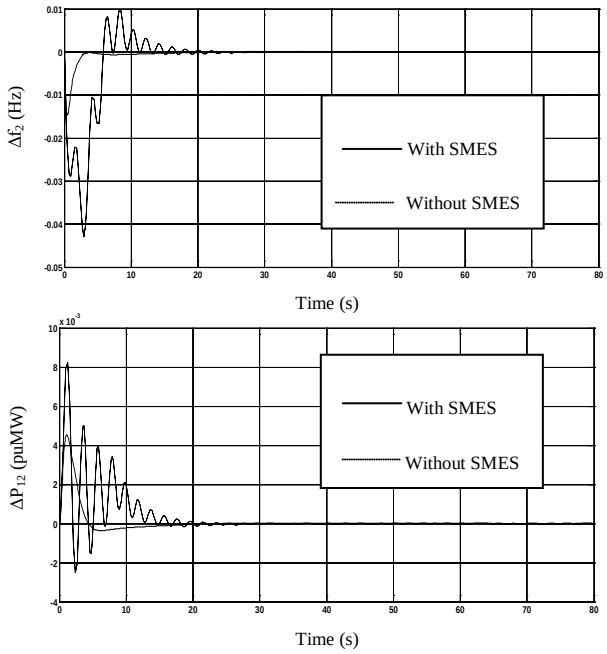

Fig.10 Dynamic responses for frequency deviations (Δf_1 & Δf_2) and tie line power deviations (ΔP_{tie12}) following 0.01 pu step load disturbance in area 2

As the load disturbance is in area 2, the generating units 1 and 2 in area 1 do not contribute for the sudden load demand as can be observed from Fig.11

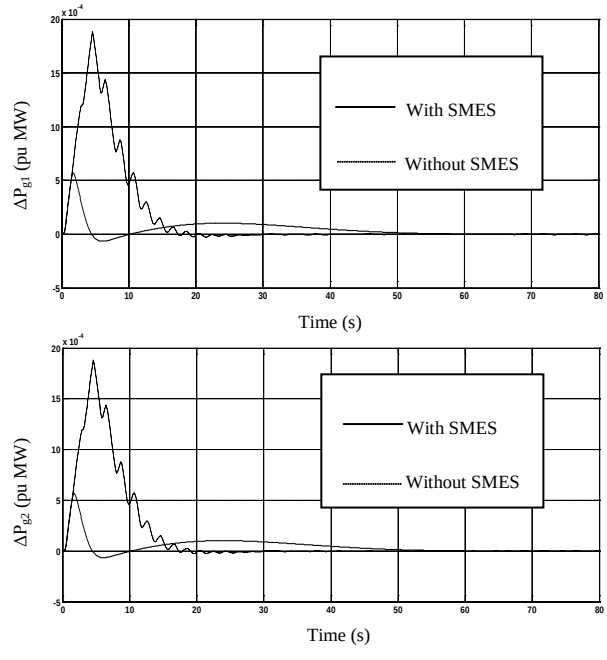

Fig.11 Dynamic responses for ΔP_{g1} and ΔP_{g2} with 0.01 pu step load disturbance in area 2

The load demand is solely met by the generating units 3 and 4 in area 2 corresponding to the area participation factors. These units equally share the load. Without and with SMES units, the change in generation in area 2 is shown in Fig.12.

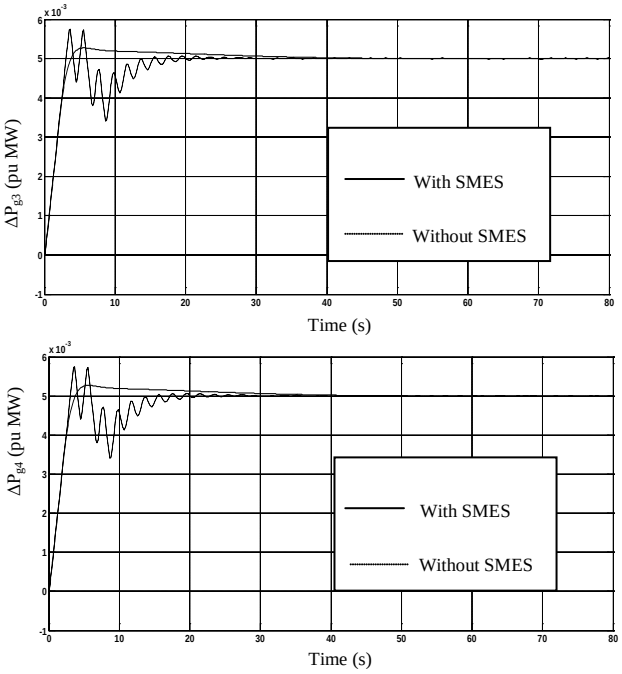

Fig.12 Dynamic responses for ΔP_{g3} and ΔP_{g4} with 0.01 pu step load disturbance in area 2

It is observed from the above responses that incorporation of SMES units into the system improves the dynamic performances. The overshoots and settling times have been considerably reduced. Effective damping of low frequency oscillations is also another advantage of using SMES units in the power system.

8 Conclusion

A small perturbation transfer function model of a two area interconnected thermal system has been modeled with a small capacity SMES unit incorporated into each area. A realistic nonlinearity constraint, generation rate constraint is also included in both the areas. A 1% step load disturbance in either of the areas has been considered for simulation. The integral gain settings were optimized using genetic algorithm considering an objective function based on integral square error criterion. Integral gain settings for different ACE participation factors with and without SMES units have been found. Simulation results reveal that with SMES, the dynamic responses have been improved in terms of overshoots and settling time when compared with those without SMES units.

Appendix

System data:
$P_{R1} = P_{R2} = 1200$ MW
$T_{P1} = T_{P2} = 20$ s
$K_{P1} = K_{P2} = 120$ Hz/p.u. MW
$T_{R1} = T_{R2} = 10$ s,
$K_{R1} = K_{R2} = 0.5$
$T_{T1} = T_{T2} = T_{T3} = T_{T4} = 0.3$ s
$T_{G1} = T_{G2} = T_{G3} = T_{G4} = 0.08$s
$R_1 = R_2 = R_3 = R_4 = 2.4$ Hz/p.u. MW
$T_{12} = 0.0866$ p.u. MW/rad., $\Delta P_{D1} = 0.01$ p.u.
$D_1 = D_2 = 8.333 \times 10\text{-}3$ p.u. MW/Hz
$B_1 = B_2 = 0.4249$ p.u. MW/Hz, $\Delta P_{D2} = 0$ p.u

SMES Parameters:
L = 2.65 H
$T_{DC} = 0.03$ s
$K_{SMES} = 100$ kV/unit MW
$K_{id} = 0.2$ kV/kA
$I_{d0} = 4.5$ kA

References:

[1] O. I. Elgerd, C. E. Fosha, Optimum megawatt frequency – control of multi-area electric energy systems, *IEEE Transactions on Power Systems*, PAS-89, 1970, pp. 556-563.

[2] C. E. Fosha, O. I. Elgerd, The megawatt frequency – control problem: A new approach via optimal control theory, *IEEE Transactions on Power Systems*, PAS-89, 1970, pp. 563-577.

[3] K. S. S. Ramakrishna, T.S. Bhatti, Automatic generation control of single area power system with multi-source power generation, *Proc. IMechE., Part A: J. Power and Energy*, 222, (1) , 2008, pp. 1-11.

[4] H. Shayeghi, H. A. Shayanfar, and A. Jalili, Load frequency control strategies: A state-of-the-art survey for the researcher, *Energy Conversion and Management*, 50, 2009, pp. 344-353.

[5] Ibraheem, P. Kumar, and D. P. Kothari, Recent philosophies of automatic generation control strategies in power systems, *IEEE Transactions on Power Systems*, 20, (1), 2005, pp. 346-357.

[6] S. Doola, T. S. Bhatti, A new load frequency control technique for an isolated small hydro power plant, *Proc. IMechE., Part A: J. Power and Energy*, 221, (1) , 2008, pp. 51-57.

[7] J. Nanda, M. L. Kothari, P. S. Satsangi, Automatic generation control of an interconnected hydrothermal system in continuous and discrete modes considering generation rate constraints, *IEE Proc*., 130, (1) , 1983, pp. 17-27.

[8] J. Nanda, M. L. Kothari, P. S. Satsangi, Sampled-data Automatic Generation Control of interconnected reheat thermal systems considering generation rate constraints, *IEEE Transactions on Power Apparatus and Systems*, 100, (5) , 1981, pp. 2334-2342.

[9] M. Aldeen, H. Trinh, Load frequency control of interconnected power systems via constrained feedback control schemes, *Comput Electr Eng*., 20, (1) 1994, pp. 71-88,.

[10] J. Nanda, B. L. Kaul, Automatic generation control of an interconnected power system, *Proc. IEE*., 125, (5), 1978, pp. 385-390.

[11] S. M. Miniesy, E. V. Bohn, Optimum load frequency continuous control with unknown deterministic power demand, *IEEE Trans Power Syst., PAS-91*, 1972, pp. 1910-5.

[12] P. Kundur, *Power system stability and control*, Tata Mc Graw Hill, India, 2006.

[13] N. Benjamin , W. Chan, Variable structure control of electric power generation, *IEEE Trans Power Syst*., PAS-101, (2) , 1982, pp. 376-80.

[14] W. Du, H. F. Wang, L. Xiao, and R. Dunn, The capability of energy storage systems to damp power system oscillations, *Proc. IMechE., Part A: J. Power and Energy*, 223, (7) , 2009, pp. 759-772.

[15] Mohd. Hasan Ali, Bin Wu, Roger A. Dougal, An overview of SMES Applications in Power and energy systems, *IEEE Transactions on Sustainable Energy*, 1,(1) , 2010, pp. 38-47.

[16] William V. Hassenzahl, Drew W. Hazelton, Brian K. Johnson, Peter Komarek, Mathias Noe, Chandra T. Reis, Electric Power Applications of Superconductivity, *Proc. of IEEE*, 92, (10) , 2004, pp. 1655-1674.

[17] S. C. Tripathy, R. Balasubramanian, P. S. Chandramohanan Nair, Adaptive Automatic Generation Control with Superconducting Magnetic Energy Storage in Power Systems, *IEEE Transactions on Energy Conversion*, 7, (3) , 1992, pp. 434-441.

[18] S. Banerjee , J. K. Chatterjee, S. C. Tripathy, Application of magnetic energy storage unit as continuous var controller, *IEEE Trans Energy Conver*., 5,(1), 1990, pp. 39-45.

[19] S. C. Tripathy, M. Kalanthar, R. Balasubramanian, Dynamics and stability of wind and diesel turbine generators with superconducting magnetic energy storage unit on an isolated power system, *IEEE Trans Energy Conver*., 6, (4) , 1991, pp. 579-85.

[20] B.C. Pal, A.H. Coonick, and D.C. Macdonald, Robust damping controller design in power systems with superconducting magnetic energy storage devices, *IEEE Trans. Power Syst*., 15, (1) , 2000, pp. 320–325.

[21] Y. L. Abdel Magid, M. M. Dawoud, Optimal AGC tuning with genetic algorithms, *Electric Power System Research*, 38, 1997, pp. 231-238.

[22] S. P. Ghosal, S. K. Goswami, Application of GA based optimal integral gains in fuzzy based active power-frequency control of non-reheat and reheat thermal generating systems, *Electric Power Systems Research*, 67, 2003, pp. 79-88.

[23] Gayadhar Panda, Sidhartha Panda and C. Ardil, Automatic Generation Control of multi-area electric energy systems using modified GA, *International Journal of Electrical and Electronics Engineering*, 4, (6) , 2010, pp. 419-427.

[24] M. Reformat, E.Kuffel, D. Woodford, and W. Pedrycz, Application of genetic algorithms for control design in power systems, *IEE Proc., Gener. Transm. Distrib.*, 145, (4) , 1998, pp. 345–354.

[25] IEEE Committee Report, *IEEE Trans. Power Apparatus and Systems*, 86, 1966, pp. 384-395.

[26] E. W. Kimbark, *Direct Current Transmission* New York: John Wiley, 1971